

Characterization of terahertz field confinement at the end of a tapered metal wire waveguide

Victoria Astley, Rajind Mendis, and Daniel M. Mittleman^{a)}

Department of Electrical and Computer Engineering, Rice University, MS 366, Houston, Texas 77251-1892, USA

(Received 14 May 2009; accepted 1 July 2009; published online 21 July 2009)

We present experimental verification of the possibility of strong subwavelength confinement of the terahertz electric field at the end of a tapered metal wire waveguide. The axial field component at the end of the tapered waveguide shows a lateral confinement that is an order of magnitude greater than an untapered waveguide, and over 100 times greater than the free-space wavelength. The axial component is also strongly confined in the propagation direction, in contrast to the radial field component. Comparison to numerical simulation yields excellent agreement when the effect of the detecting probe is included in the analysis. © 2009 American Institute of Physics.

[DOI: 10.1063/1.3186065]

The use of waveguides for the focusing of electromagnetic energy has been an important avenue to achieving sub-wavelength resolution in near-field imaging. There is considerable interest in a method of confining electromagnetic radiation without suffering the high loss and dispersion of aperture-based techniques or the low image contrast of apertureless techniques. By using a plasmonic waveguide to obtain subwavelength focusing of radiation, these problems could potentially be avoided.

A variety of surface-plasmon waveguides have been used for superfocusing applications, such as a coaxial conical horn microwave antenna,¹ metal nanoparticle chains,² metal or metal-coated wedges,³ metal nanowires,⁴ waveguides with gap plasmons,⁵ metal-coated optical fiber tips,⁶ and tapered metal stripes.⁷ Of particular interest are tapered metallic wires,^{8–10} in which a metal wire guides a surface plasmon to a tapered conical tip. The size of the propagating surface wave tapers along with the waveguide diameter, resulting in subwavelength confinement of electromagnetic energy at the tip. Simulations at the nanoscale for visible wavelengths predict an intensity increase of three orders of magnitude at the end of the waveguide,⁹ though the enhancement is dependent on factors such as the wavelength, the taper angle, the waveguide material, and the tip radius.¹¹

In the terahertz region of the spectrum, tapered wire waveguides are particularly promising because of the recent recognition of the efficiency of bare metal wires as broadband waveguides.¹² Both analytic theory¹³ and numerical simulations^{14–16} at terahertz frequencies indicate subwavelength confinement at the tip of the taper. Experimental confirmation has been limited due to the difficulty of observing this confinement directly but initial results support the predictions of field enhancement in the region of the tip.^{16–18} Based on these results, tapered wires for terahertz near-field imaging and spectroscopy have begun to be implemented with promising results.^{19–21}

However, there has been no direct experimental study of the efficacy of confining a guided terahertz surface (Sommerfeld) wave using a tapered wire. Without such a direct obser-

vation, the implementation of tapered waveguides as near-field probes or high-intensity localized terahertz plasmons^{9,22} is shaped by the assumed accuracy of simulations, which have not been compared to experimental data.

Here, we employ a technique we recently developed, scattering-probe imaging,²³ to provide experimental characterization of the subwavelength confinement. We use a sharp metal probe tip, similar to those used in apertureless near-field microscopy, to sample the electric field in the immediate vicinity of the tip. The component of the electric field polarized parallel to the probe axis at the position of the tip of the probe is detected in the far field, with resolution limited by the tip size.

A schematic of the experimental setup is shown in Fig. 1. A radially symmetric photoconductive antenna²⁴ is used to generate broadband radially polarized picosecond terahertz pulses, which are then coupled onto a 500 μm diameter stainless steel cylindrical wire waveguide. A tungsten scattering probe with a tip diameter of 20 μm is placed with its tip at the end of the waveguide and its axis along the direction of propagation (the z axis), a configuration which is sensitive only to the z component of the electric field. The terahertz radiation propagates along the waveguide, then couples into free space and scatters off the probe tip. The scattered radi-

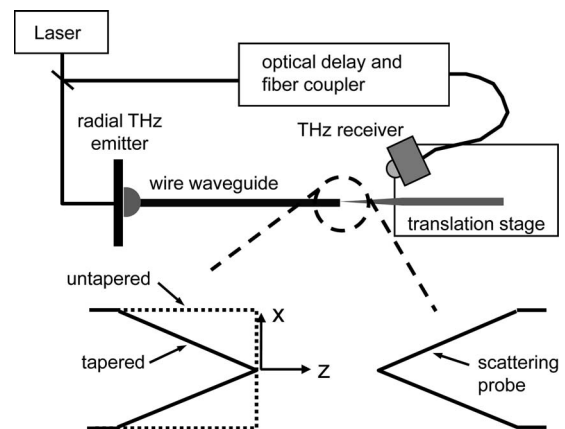


FIG. 1. Schematic of the experimental setup. Radially polarized terahertz radiation is coupled directly to a wire waveguide, and detected at the opposite end using a scattering-probe geometry.

^{a)}Author to whom correspondence should be addressed. Electronic mail: daniel@rice.edu.

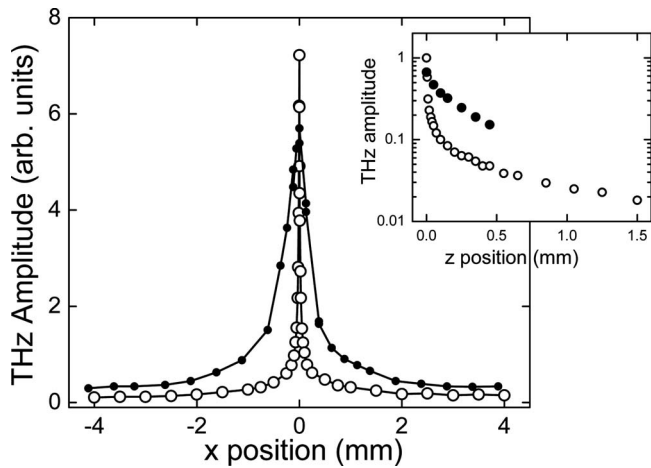


FIG. 2. One-dimensional (along the x direction) plot of the peak-to-peak amplitude of the z component of the terahertz electric field at the end of the untapered (solid circles) and tapered (open circles) waveguides. The field confinement for the tapered waveguide is comparable to the size of the tip, roughly 20 times smaller than in the untapered case, and over 100 times less than the average free-space wavelength. The inset shows the power-law decay of the field along the z axis for the tapered and untapered waveguides.

tion is detected in the far field using a fiber-coupled photoconductive dipole antenna. This receiver is 90° out of plane, to reduce any asymmetry effects due to receiver positioning.²³ Both the probe and the receiver are placed on a two-axis translation stage, in order to measure the z component of the terahertz electric field, E_z , in the region just beyond the end of the waveguide. For sensitive detection, the probe is mounted on a piezoelectric transducer which shakes it in the z direction with an amplitude of $10\ \mu\text{m}$ and a frequency of 160 Hz. This modulation, which serves as the reference for lock-in detection, greatly increases the signal-to-noise of the obtained data, removes background, and ensures that the detected signal originates only from scattering at the probe tip.

Using this procedure, we map the field at the end of two different wire waveguides, one with a flat end, and the second with a taper. For this latter case, the cone angle of the taper is 4.7° and the tip diameter is $20\ \mu\text{m}$. The data obtained in this fashion are compared to the results of finite-element-method (FEM) simulations performed at 100 GHz.

By scanning the probe in one dimension, we sample E_z at various points along a line, for both the untapered and tapered waveguides. Figure 2 shows these results for scans along the x direction, perpendicular to the waveguide axis, with the probe tip at closest approach ($z \approx 0$). For the untapered waveguide, the full width at half maximum (FWHM) of this field distribution is approximately $630\ \mu\text{m}$, which is roughly equal to the waveguide diameter. In contrast, the FWHM for the tapered waveguide is approximately $30\ \mu\text{m}$, comparable to the tip size, more than an order of magnitude smaller than that of the untapered waveguide, and 100 times less than the average free-space wavelength. The inset shows the results for a scan along the z direction (parallel to the waveguide axis), again showing much stronger field confinement for E_z in the case of the tapered waveguide. This is in contrast to the radial component of the electric field, which is predicted to show high confinement only at the tip of the waveguide, before strongly diffracting, once the energy escapes into free space.¹⁴ The decay of the signal with increas-

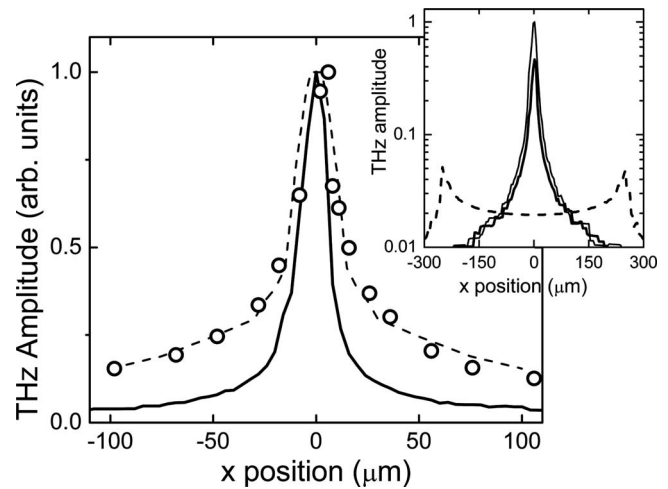


FIG. 3. A comparison of measured and simulated one-dimensional field patterns along the x direction. The open circles denote the experimentally measured values at 100 GHz, extracted from the time-domain waveforms by Fourier transform. The solid black line is the result of a single FEM simulation, showing the value of E_z at $z=5\ \mu\text{m}$ beyond the end of the tip. The dashed line is extracted from a series of FEM simulations, each including both the tapered waveguide and the scattering probe. This shows the effect of the field strengthening that results from the presence of the probe. All three curves have been normalized for comparison. Inset: a comparison of three FEM simulations, showing the case of an untapered wire with abrupt planar termination (dashed curve), a tapered wire (thick curve), and a tapered wire with a second probe tip located on axis with its tip situated at $z=10\ \mu\text{m}$ (thin curve). Tapering the waveguide leads to a field enhancement (on-axis) of about a factor of 10, relative to the untapered waveguide. Adding a second metal tip leads to an additional field enhancement of about a factor of 2.

ing z follows a power law, as expected for a conical metal tip.^{11,25}

In order to understand the limits of this field confinement, we make quantitative comparisons using the results of our FEM simulations. These simulations use metal tips with similar geometry to those used in the experiments, and with surface impedance set equal to that of copper. By Fourier transforms of the measured time-domain waveforms, we extract the amplitude of the terahertz field at 100 GHz. These experimental results and simulations are compared in Fig. 3. At 100 GHz, the experimental FWHM (circles) is $31\ \mu\text{m}$, whereas the simulation (solid curve) indicates a higher field confinement, with a FWHM of $17\ \mu\text{m}$. This difference, roughly a factor of 2, could result from experimental considerations, such as an incorrect measurement of the ($z \approx 0$) point of closest approach or a misalignment of the location of the probe in a direction orthogonal to the waveguide axis. Or, more interestingly, the discrepancy could result from the fact that the probe modifies the field confinement. This modification would arise from the distortion of the charge distribution in the metal waveguide induced by the nearby metal sampling probe. In analogy to the formation of an image dipole when a metal object is close to a ground plane, this would strengthen the field at the tip of the waveguide relative to the field without the probe. This is essentially equivalent to the well-known “height artifact” of apertureless near-field microscopy,²⁶ and could lead to an inaccurate estimation of the field confinement at the tip of an isolated tapered waveguide.

To investigate this latter possibility, we have performed a series of additional FEM simulations. These results (inset

to Fig. 3) show $|E_z|$ as a function of x at a distance of $z=5 \mu\text{m}$ beyond the end of the waveguide. The dashed curve shows the result for an untapered waveguide, exhibiting small peaks at $x=\pm 250 \mu\text{m}$, the positions corresponding to the locations of the two (in the simulations, perfectly sharp) corners where the cylindrical wire terminates. The tapered waveguide (thick solid curve) shows a dramatic (factor of 10) field enhancement at $x=0$, and a correspondingly high field confinement. In the third simulation (thin solid curve), we add a *second* tapered metal structure on axis, representing the probe, at a position $z=10 \mu\text{m}$ from the waveguide. This clearly shows an additional strengthening of the field, roughly by a factor of 2 at $x=0$. These results indicate that the presence of the probe has some effect on the measured field enhancement and field confinement.

To disentangle this apparent strengthening of the measured field at the tip of the tapered-wire waveguide, we perform a series of additional simulations, in which the scattering probe is included at $z=10 \mu\text{m}$ at various offset positions along the x direction. At each offset, we extract the value of E_z at a position $5 \mu\text{m}$ from the end of the probe. This procedure accounts for the additional field strengthening, as well as its dependence on the lateral (x) offset of the probe. These results, shown as a dashed curve in Fig. 3, show much better agreement with the experimental results at 100 GHz. As a result, we conclude that the measured field confinement of $\sim 30 \mu\text{m}$, in fact, corresponds to a true field confinement of less than $20 \mu\text{m}$ in the absence of the scattering probe, about equal to the waveguide tip diameter.

In conclusion, we have experimentally confirmed the subwavelength confinement of the z component of the electric field at the end of a tapered metal wire waveguide in agreement with numerical simulations. The scale of the lateral confinement is tip-size limited, and more than 100 times smaller than the free-space wavelength. This result supports the use of tapered waveguides for terahertz near-field imaging and for creating high-intensity localized terahertz surface plasmons using tapered wires. We have also established that the presence of a (detecting) scattering probe can modify the apparent degree of field confinement, and must be considered for a quantitative analysis.

This work was supported in part by the National Science Foundation, and by the Lockheed Martin Advanced Nanotechnology Center of Excellence at Rice University (LANCER). V.A. gratefully acknowledges support from the National Defense Science and Engineering Graduate Fellowship program.

- ¹F. Keilmann, *Infrared Phys. Technol.* **36**, 217 (1995).
- ²S. A. Maier, P. G. Kik, H. A. Atwater, S. Meltzer, E. Harel, B. E. Koel, and A. A. G. Requicha, *Nature Mater.* **2**, 229 (2003).
- ³T. Yatsui, M. Kurogi, and M. Ohtsu, *Appl. Phys. Lett.* **79**, 4583 (2001).
- ⁴J. R. Krenn, B. Lamprecht, H. Ditlbacher, G. Schider, M. Salerno, A. Leitner, and F. R. Aussenegg, *Europhys. Lett.* **60**, 663 (2002).
- ⁵D. F. P. Pile and D. K. Gramotnev, *Appl. Phys. Lett.* **89**, 041111 (2006).
- ⁶N. A. Janunts, K. S. Baghdasaryan, K. V. Nerkararyan, and B. Hecht, *Opt. Commun.* **253**, 118 (2005).
- ⁷E. Verhagen, A. Polman, and L. K. Kuipers, *Opt. Express* **16**, 45 (2008).
- ⁸F. Keilmann, *J. Microsc.* **194**, 567 (1999).
- ⁹M. I. Stockman, *Phys. Rev. Lett.* **93**, 137404 (2004).
- ¹⁰C. Ropers, C. C. Neacsu, M. B. Raschke, M. Albrecht, C. Lienau, and T. Elsaesser, *Jpn. J. Appl. Phys.* **47**, 6051 (2008).
- ¹¹A. V. Goncharenko, J.-K. Wang, and Y.-C. Chang, *Phys. Rev. B* **74**, 235442 (2006).
- ¹²K. Wang and D. M. Mittleman, *Nature (London)* **432**, 376 (2004).
- ¹³H. Liang, S. Ruan, and M. Zhang, *Opt. Express* **16**, 18241 (2008).
- ¹⁴J. A. Deibel, N. Berndsen, K. Wang, D. M. Mittleman, N. C. J. van der Valk, and P. C. M. Planken, *Opt. Express* **14**, 8772 (2006).
- ¹⁵S. A. Maier, S. R. Andrews, L. Martin-Moreno, and F. J. Garcia-Vidal, *Phys. Rev. Lett.* **97**, 176805 (2006).
- ¹⁶Y. B. Ji, E. S. Lee, J. S. Jang, and T.-I. Jeon, *Opt. Express* **16**, 271 (2008).
- ¹⁷N. C. J. van der Valk and P. C. M. Planken, *Appl. Phys. Lett.* **81**, 1558 (2002).
- ¹⁸A. J. L. Adam, N. C. J. van der Valk, and P. C. M. Planken, *J. Opt. Soc. Am. B* **24**, 1080 (2007).
- ¹⁹P. C. M. Planken, C. E. W. M. van Rijmenam, and R. N. Schouten, *Semicond. Sci. Technol.* **20**, S121 (2005).
- ²⁰H. Zhan, V. Astley, M. Hvasta, J. A. Deibel, D. M. Mittleman, and Y.-S. Lim, *Appl. Phys. Lett.* **91**, 162110 (2007).
- ²¹M. Awad, M. Nagel, and H. Kurz, *Appl. Phys. Lett.* **94**, 051107 (2009).
- ²²A. J. Huber, F. Keilmann, J. Wittborn, J. Aizpurua, and R. Hillenbrand, *Nano Lett.* **8**, 3766 (2008).
- ²³V. Astley, H. Zhan, R. Mendis, and D. M. Mittleman, *J. Appl. Phys.* **105**, 113117 (2009).
- ²⁴J. A. Deibel, K. Wang, M. D. Escarra, and D. M. Mittleman, *Opt. Express* **14**, 279 (2006).
- ²⁵H. Cory, A. C. Boccara, J. C. Rivoal, and A. Lahrech, *Microwave Opt. Technol. Lett.* **18**, 120 (1998).
- ²⁶B. Knoll and F. Keilmann, *Opt. Commun.* **182**, 321 (2000).